Four-Loop Nonsinglet Splitting Functions in QCD

Thomas Gehrmann,[1,*] Andreas von Manteuffel,[2,†] Vasily Sotnikov,[1,‡] and Tong-Zhi Yang[3,4,§]
[1]Physik-Institut, Universität Zürich, Winterthurerstrasse 190, 8057 Zürich, Switzerland
[2]Institut für Theoretische Physik, Universität Regensburg, 93040 Regensburg, Germany
[3]State Key Laboratory of Nuclear Physics and Technology, Institute of Quantum Matter, South China Normal University, Guangzhou 510006, China
[4]Guangdong Basic Research Center of Excellence for Structure and Fundamental Interactions of Matter, Guangdong Provincial Key Laboratory of Nuclear Science, Guangzhou 510006, China

(Received 23 April 2026; revised 19 June 2026; accepted 13 August 2026; published 18 November 2026)

The scale evolution of parton distributions is governed by splitting functions. We compute the four-loop splitting functions in perturbative QCD that control the evolution of quark nonsinglet distributions. We confirm previous partial results and obtain, for the first time, fully analytic expressions for all nonsinglet contributions at this order. These allow us to extract the analytic form of the four-loop virtual and rapidity anomalous dimensions entering logarithmic resummation. We provide precise numerical representations of the splitting functions suitable for parton evolution.

DOI: 10.1103/sgtd-c4zg

Introduction—The proton is a complex bound state of quarks and gluons. Its inner structure is encoded in parton distribution functions (PDFs), which describe [1,2] the probability of finding a quark, antiquark, or gluon carrying a fraction x of the proton's momentum when probing it at a resolution scale Q^2. The PDFs encode the nonperturbative bound state dynamics of the proton; they are universal quantities appearing in the calculation of any collider process involving hadrons in the initial state. Their Q^2 evolution is predicted in perturbative QCD by the Dokshitzer–Gribov–Lipatov–Altarelli–Parisi (DGLAP) equations [3–5], which form a coupled set of integrodifferential equations. The kernels of the DGLAP equations are the splitting functions $P(x)$, which determine the probability of partons transitioning into each other while transferring a given fraction x of their longitudinal momentum.

The splitting functions can be computed in a loop expansion in QCD perturbation theory, and their knowledge to a given order enables the extraction of PDFs accurate to this order from a global fit to experimental data from a wealth of processes in lepton-hadron and hadron-hadron collisions. Analytical expressions for the splitting functions were derived at one loop [3,6,7], two loops [8–13], and three loops [14–18], enabling PDF fits at leading order (LO), next-to-leading order (NLO) and next-to-next-to-leading order (NNLO), respectively. At four loops, approximate expressions for the splitting functions [19–25] as well as partial analytical results [26–32] are available, which are already being used in PDF determinations at next-to-next-to-next-to-leading order (N^{3}LO) [33–38]. The approximate four-loop splitting functions may be sufficient for many phenomenological applications. Knowledge of their complete analytical expressions is nevertheless highly desirable since it will enable the elimination of the approximation uncertainty and allows for in-depth analytical studies of their asymptotic behavior at large and small x.

For n_f quark flavors, the $(2n_f+1)$ DGLAP evolution equations can be decoupled by introducing $(2n_f-2)$ flavor-asymmetric nonsinglet combinations of the form

$$q^{\pm}_{\mathrm{ns},ij} = q_i \pm \bar{q}_i - (q_j \pm \bar{q}_j) \tag{1}$$

and one nonsinglet valence sum distribution,

$$q^{V}_{\mathrm{ns}} = \sum_i (q_i - \bar{q}_i), \tag{2}$$

thus leaving a system of two coupled equations for the quark singlet and the gluon. In this Letter, we compute analytical expressions for the three different four-loop splitting functions $P^{\pm,V}_{\mathrm{ns}}$, with $P^{V}_{\mathrm{ns}} = P^{-}_{\mathrm{ns}} + P^{s}_{\mathrm{ns}}$, that govern the evolution of the different nonsinglet quark distributions. These spacelike splitting functions directly determine [19,39–41] their timelike counterparts, which describe the evolution of nonsinglet hadron fragmentation functions.

*Contact author: thomas.gehrmann@uzh.ch
†Contact author: manteuffel@ur.de
‡Contact author: vasily.sotnikov@physik.uzh.ch
§Contact author: tongzhi.yang@m.scnu.edu.cn

Published by the American Physical Society under the terms of the Creative Commons Attribution 4.0 International license. Further distribution of this work must maintain attribution to the author(s) and the published article's title, journal citation, and DOI. Funded by SCOAP^3.

Methodology—The QCD splitting functions $P(x)$ relate to the anomalous dimensions $\gamma(n)$ of quark and gluon operators through the Mellin transformation:

$$\gamma(n) = -\int_0^1 dx\, x^{n-1} P(x). \tag{3}$$

The splitting functions can, therefore, be extracted from the anomalous dimensions $\gamma(n)$ for symbolic Mellin moments n. These are determined in the operator product expansion from the respective two-parton operator matrix elements (OME) in off-shell kinematics [6,7]. In the nonsinglet case, we compute

$$A_{\rm ns} = \langle q(p)|O_{\rm ns}|q(p)\rangle, \quad \text{with} \quad p^2 < 0. \tag{4}$$

The twist-two operator of spin n,

$$O_{\rm ns}(n) = \frac{i^{n-1}}{2}\bar{\psi}\Delta\cdot\gamma(\Delta\cdot D)^{n-1}\frac{\lambda}{2}\psi, \tag{5}$$

contains the flavor space matrices λ, which project onto the different nonsinglet quark combinations. Here, covariant derivatives D_μ and Dirac matrices γ_μ are contracted with a lightlike auxiliary vector Δ_μ to create a scalar operator.

The renormalization of the nonsinglet operators takes a multiplicative form,

$$O^{\rm R}_{\rm ns}(\mu, n) = Z_{\rm ns}(\mu, n) O^{\rm B}_{\rm ns}(n), \tag{6}$$

with $O^{\rm B}$ and $O^{\rm R}$ denoting the bare and renormalized operators, respectively. This simple multiplicative renormalization is in stark contrast to the quark singlet sector, which mixes with the gluon operator and with further gauge-variant operators, leading to a conceptually involved renormalization pattern [6,13,42] that could be fully understood only quite recently [18,43–45].

The anomalous dimension $\gamma_{\rm ns}$ is defined through

$$\frac{dZ_{\rm ns}(\mu, n)}{d\ln\mu} = -2\gamma_{\rm ns}(\mu, n) Z_{\rm ns}(\mu, n). \tag{7}$$

Its perturbative expansion in the renormalized coupling $a_s = \alpha_s(\mu)/(4\pi)$ reads

$$\gamma_{\rm ns} = \sum_{l=0}^{\infty} a_s^{l+1} \gamma_{\rm ns}^{(l)}, \tag{8}$$

where $\gamma_{\rm ns}^{(l)}$ is the $(l+1)$ loop contribution. The dependence on the Mellin moment index n is omitted for brevity. Employing dimensional regularization in $4-2\epsilon$ dimensions, one can extract the anomalous dimensions from the single ϵ-pole terms of renormalization constants $Z_{\rm ns}(\mu, n)$.

At one-loop order, all three nonsinglet anomalous dimensions agree with each other. $\gamma_{\rm ns}^-$ and $\gamma_{\rm ns}^+$ differ from two loops onward, and $\gamma_{\rm ns}^V$ deviates from $\gamma_{\rm ns}^-$ starting at three loops.

To compute the four-loop anomalous dimensions, we calculate Feynman diagrams for matrix elements (4) with two external quarks and an operator insertion on a quark line. We generate $\mathcal{O}(16\,\text{k})$ diagrams with `Qgraf` [46], from which we select the ones contributing to the nonsinglet anomalous dimensions. Example diagrams are shown in Fig. 1.

We perform the Lorentz, Dirac, and color algebra with `Form` [47,48] and `Color.h` [49]. For an operator of spin

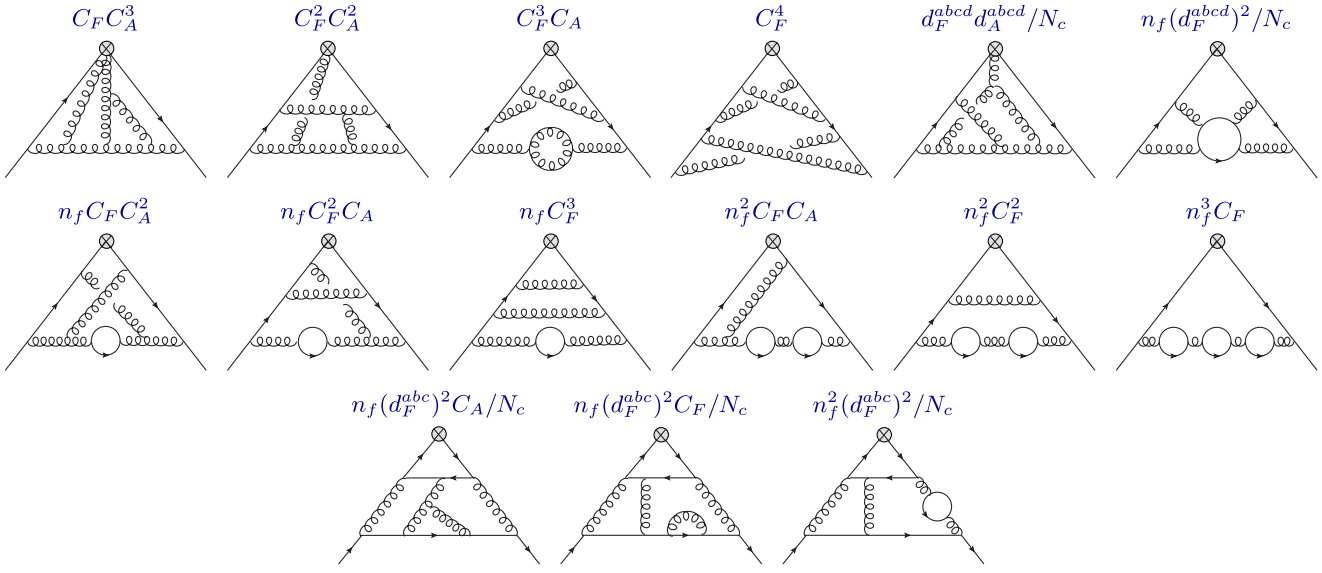


FIG. 1. Sample Feynman diagrams for off-shell quark self-energies with an operator insertion (crossed vertex) contributing to different color coefficients of the splitting functions $P_{\rm ns}^{(3)\pm}$ (upper two rows) and $P_{\rm ns}^{(3)s}$ (lower row) at four loops. Both planar and nonplanar diagrams contribute. The operator insertion may involve up to four gluons (curly lines) in addition to the two quarks (straight lines).

n, the corresponding Feynman rule gives rise to terms like $(\Delta \cdot k)^{n-1}$, where k is the momentum of any particle adjacent to the operator. These symbolic powers in numerator insertions can be transformed into linear propagators by the introduction of an auxiliary parameter t [50,51]. For example, we replace

$$(\Delta \cdot k)^{n-1} \to \sum_{n=1}^{\infty} t^n (\Delta \cdot k)^{n-1} = \frac{t}{1 - t\Delta \cdot k}, \tag{9}$$

thus allowing us to perform symbolic manipulations and reexpand the final result to extract the contribution for a specific value n.

The resulting scalar Feynman integrals can be indexed by 52 complete sets of standard and linear propagators (integral families) and assigned to 549 top-level sectors with 13 different propagators and their subsectors. Here, a sector refers to a set of different propagator denominators. We encounter $\mathcal{O}(3\ \mathrm{M})$ unreduced integrals with at most 13 different propagators. Using momentum shift relations, this number reduces to $\mathcal{O}(260\ \mathrm{k})$ integrals, with up to five irreducible scalar products in the numerator and up to four repeated propagators ("dots"). We employ integration-by-parts (IBP) reductions [52,53] with `Reduze 2` [54] and the private code `Finred`. Standard IBP relations reduce the matrix elements in terms of $\mathcal{O}(120\ \mathrm{k})$ integrals. Taking also shift relations between sectors, discrete symmetry relations within sectors, and certain anomalous IBP identities generated in supersectors into account, one can express all integrals in terms of $\mathcal{O}(6\ \mathrm{k})$ master integrals.

For the matrix element reduction, we employ standard momentum-space IBP relations with finite field sampling [55,56] and a custom implementation to optimize the selection of equations; see also [57–62]. For a given top-level sector, we determine a set of spanning sectors [58,63] and sample the reduced matrix element for each of them. In total, we probe $\mathcal{O}(9\ \mathrm{k})$ spanning sectors. We make an effort to avoid the introduction of denominator factors with mixed ϵ and t dependence through the choice of the basis integrals [64,65]. After guessing denominators and simple numerator factors [66,67], we reconstruct the reduced matrix element from finite field samples.

To find the solutions of the basis integrals, we derive differential equations (DEs) [68,69] with respect to the tracing parameter t for $\mathcal{O}(300)$ top-level sectors. For each top-level sector τ, we obtain

$$\partial_t I^\tau = A^\tau(\epsilon, t) I^\tau, \tag{10}$$

where the vector I^τ contains the basis integrals and $A^\tau(\epsilon, t)$ is a matrix. One fifth of all DEs have dimension larger than 900, with the two largest ones exceeding 2000, and homogeneous coupled blocks of size 12 are commonly encountered.

We derive Laurent series solutions in ϵ with coefficients that are Taylor series in t as follows. From the DEs, we derive recursion relations for series coefficients of each integral [70–72]. The solutions of interest to us are required to be regular in the limit $t \to 0$. Moreover, in the limit $t \to 0$, all integrals are reduced to a basis of 28 standard self-energy integrals [73–76], which fix all boundary conditions. We expand the boundary integrals to sufficiently high orders in ϵ such that contributions up to weight 7 to the OMEs are fully captured.

We use the recursion relations to obtain a sufficient number of t powers for all integrals, which allows us to compute the four-loop bare OMEs up to $\mathcal{O}(4000)$ moments. From these moments, we successfully reconstruct the four-loop anomalous dimensions $\gamma_{\mathrm{ns}}^{(3)}$ in terms of harmonic sums [77], employing the renormalization formula (6) and lower-order OME counterterms [18]. Unlike the strong constraints imposed in [19,31], our n-space reconstruction uses a generic ansatz: for $\gamma_{\mathrm{ns}}^{(3)\pm}$, harmonic sums up to weight 7 and two denominator structures $\{n, n+1\}$; for $\gamma_{\mathrm{ns}}^{(3)s}$, harmonic sums up to weight 6 and five denominator structures $\{n, n+1, n-1, n+2, n-2\}$.

While our method of solving DEs by Taylor expansion in t is not particularly concerned with the structure of rational matrices $A^\tau(\epsilon, t)$, we studied the closed-form solutions of their homogeneous blocks $\hat{A}_i^\tau(\epsilon, t)$ in more detail for some examples. In addition to square root solutions that do not appear in a three-loop computation, we also surprisingly find that integrals related to elliptic geometry appear at four loops for the first time. For example, for the integrals with denominators shown in Fig. 2, we initially find a 4×4 homogeneous coupled DE $B_e = \hat{A}_e^\tau(0, t)$. Using a private extension of the package `DLogBasis` [78], we obtain two candidates that have dlog integrands in four-dimensional momentum parametrization, which decouple from B_e. We convert the remaining 2×2 system into a second-order DE whose solutions are periods of an elliptic curve. We then use the ansatz method of [79] to find an ϵ-factorized form with a transformation that contains complete elliptic integrals of the first and second kind. Interestingly, if one were to derive exact solutions in t, instead of the Taylor series solutions here, the iterated integrals with elliptic kernels originating from such Feynman integrals are expected to completely drop out from the poles in ϵ of the

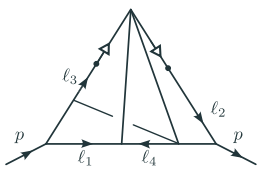


FIG. 2. Feynman integral topology with 11 denominators associated with elliptic geometry. This topology occurs as a subtopology of the fifth diagram in Fig. 1. The lines marked with hollow triangles and dots correspond to insertions of denominators $1 - t(\Delta \cdot \ell_i)$ with tracing parameter t in addition to standard (quadratic) propagators.

bare OME result since we are able to recover the all-n result expressed through harmonic sums.

Results—Our analytic results for $\gamma_{\rm ns}^{(3)}$ are expressed solely in terms of harmonic sums and decomposed into 15 color structures, as shown in Fig. 1, with

$$\begin{aligned} &T = 1/2, \qquad C_A = 3, \qquad C_F = 4/3, \\ &(d_F^{abc})^2/N_c = 5/18, \\ &d_F^{abcd} d_A^{abcd}/N_c = 5/2, \qquad (d_F^{abcd})^2/N_c = 5/36 \end{aligned} \tag{11}$$

for the $SU(3)$ gauge group of QCD. The nonfermionic contributions to $\gamma_{\rm ns}^{(3)\pm}$ and the n_f term in $\gamma_{\rm ns}^{(3)s}$, represented by the first five structures in the top row and the first two in the bottom row of Fig. 1, are obtained here for the first time. Analytic results for other color structures (including the leading color) were initially derived in [19,26,27,29,31] and are confirmed here. By evaluating our results with fixed n, we found full agreement with fixed moment results in [19]. We observed that the harmonic sums of weight 6 and denominator structure $\{n-2\}$ in the n-space ansatz drop out for $\gamma_{\rm ns}^{(3)s}$; however, the result does contain terms like $S_{1,1,-3}(n)/n^2$, which is weight 7 if we count the $1/n^2$ as weight 2.

By performing an inverse Mellin transformation with respect to Eq. (3), as implemented in the `HarmonicSums` package [80,81], the corresponding analytic four-loop nonsinglet splitting functions are obtained. The results contain harmonic polylogarithms [82,83] up to weight 6 and transcendental constants up to weight 7, appearing in the $\delta(1-x)$ part of $P_{\rm ns}^{(3)\pm}$. For numerical evaluations and expansions of the harmonic polylogarithms, we employ the package `HPL` [84] and the implementation [85] of G functions in `GiNaC`.

Our analytic results allow us to study the asymptotic behavior of the splitting functions. In the limit of $x \to 1$, $P_{\rm ns}^{(3)s}$ vanishes at leading and next-to-leading power. The $P_{\rm ns}^{(3)+}$ and $P_{\rm ns}^{(3)-}$ are identical to next-to-leading power and can be written as

$$\begin{aligned} P_{\rm ns}^{(3)\pm} = {} & A_4 \left[\frac{1}{1-x}\right]_+ + B_4 \delta(1-x) \\ & + C_4 \log(1-x) + D_4 - A_4 + \mathcal{O}(1-x), \end{aligned} \tag{12}$$

where $[\ ]_+$ denotes the plus distribution [3,86]. The A_4 is the four-loop cusp anomalous dimension [87], derived in [88,89], where we find full agreement. The B_4 is called four-loop virtual anomalous dimension, and we obtain its analytic form here for the first time:

$$\begin{aligned} B_4 = {} & C_A^3 C_F \left(-\frac{8960}{3}\zeta_7 + \frac{1472}{3}\zeta_5\zeta_2 + \frac{32}{3}\zeta_4\zeta_3 + \frac{73\,333}{108}\zeta_6 + \frac{1672}{3}\zeta_3^2 + \frac{11\,522}{9}\zeta_5 + \frac{584}{3}\zeta_3\zeta_2 - \frac{11\,206}{27}\zeta_4 - \frac{152\,284}{81}\zeta_3 \right. \\ & \left. + \frac{13\,864}{9}\zeta_2 - \frac{373\,793}{648} \right) + C_A^2 C_F^2 \left(8610\zeta_7 - 2104\zeta_5\zeta_2 - 32\zeta_4\zeta_3 - \frac{5497}{2}\zeta_6 - \frac{7102}{3}\zeta_3^2 + \frac{5354}{9}\zeta_5 + \frac{2096}{9}\zeta_3\zeta_2 \right. \\ & \left. - \frac{60\,850}{27}\zeta_4 + \frac{129\,662}{27}\zeta_3 - \frac{46\,771}{27}\zeta_2 + \frac{29\,639}{36} \right) + C_A C_F^3 \left(-10\,920\zeta_7 + 2064\zeta_5\zeta_2 + 128\zeta_4\zeta_3 + \frac{79\,297}{18}\zeta_6 \right. \\ & \left. + 3220\zeta_3^2 - 976\zeta_5 - \frac{1988}{3}\zeta_3\zeta_2 + 2167\zeta_4 - 3260\zeta_3 + 1167\zeta_2 - \frac{2085}{4} \right) + C_F^4 \left(5880\zeta_7 - 384\zeta_5\zeta_2 \right. \\ & \left. + 64\zeta_4\zeta_3 - 2111\zeta_6 - 1152\zeta_3^2 - 2520\zeta_5 - 120\zeta_3\zeta_2 - 342\zeta_4 + 2004\zeta_3 - 450\zeta_2 + \frac{4873}{24} \right) + \frac{d_F^{abcd} d_A^{abcd}}{N_c} \left(2800\zeta_7 \right. \\ & \left. + 320\zeta_5\zeta_2 - 64\zeta_3\zeta_4 - \frac{1562}{9}\zeta_6 - 704\zeta_3^2 - 400\zeta_5 - 896\zeta_3\zeta_2 + \frac{32}{3}\zeta_4 - \frac{1232}{3}\zeta_3 - \frac{944}{3}\zeta_2 + 96 \right) + C_A^2 C_F n_f \left(-\frac{3913}{27}\zeta_6 \right. \\ & \left. + \frac{416}{3}\zeta_3^2 + \frac{1130}{9}\zeta_5 - \frac{580}{3}\zeta_3\zeta_2 + \frac{1234}{9}\zeta_4 + \frac{9554}{27}\zeta_3 - \frac{41\,092}{81}\zeta_2 + \frac{20\,027}{108} \right) + C_A C_F^2 n_f \left(351\zeta_6 - \frac{1232}{3}\zeta_3^2 \right. \\ & \left. - \frac{7432}{9}\zeta_5 + \frac{2672}{9}\zeta_3\zeta_2 + \frac{27\,854}{27}\zeta_4 - \frac{15\,400}{27}\zeta_3 - \frac{3892}{27}\zeta_2 - \frac{7751}{54} \right) + C_F^3 n_f \left(-\frac{6434}{9}\zeta_6 + 224\zeta_3^2 + 912\zeta_5 - \frac{256}{3}\zeta_3\zeta_2 \right. \\ & \left. - 204\zeta_4 - 308\zeta_3 + 162\zeta_2 + 32 \right) + \frac{(d_F^{abcd})^2 n_f}{N_c} \left(\frac{1792}{9}\zeta_6 + 256\zeta_3^2 - 1120\zeta_5 + 64\zeta_3\zeta_2 - \frac{352}{3}\zeta_4 - \frac{992}{3}\zeta_3 + \frac{1888}{3}\zeta_2 \right. \\ & \left. - 192 \right) + C_A C_F n_f^2 \left(-\frac{88}{9}\zeta_5 + \frac{80}{3}\zeta_3\zeta_2 - \frac{80}{9}\zeta_4 - \frac{320}{9}\zeta_3 + \frac{3170}{81}\zeta_2 - \frac{193}{54} \right) + C_F^2 n_f^2 \left(\frac{368}{9}\zeta_5 - \frac{160}{9}\zeta_3\zeta_2 - \frac{2104}{27}\zeta_4 \right. \\ & \left. + \frac{56}{27}\zeta_3 + \frac{1244}{27}\zeta_2 - \frac{188}{27} \right) + C_F n_f^3 \left(-\frac{32}{27}\zeta_4 + \frac{304}{81}\zeta_3 + \frac{32}{81}\zeta_2 - \frac{131}{81} \right). \end{aligned} \tag{13}$$

Approximate numerical results for B_4 have been presented in [90]; they are in good agreement with the analytical result above. Together with the four-loop collinear anomalous dimension [89,91] appearing in the quark form factor, our result for B_4 yields an analytic determination of the four-loop soft anomalous dimension, the eikonal quantity [92–95] controlling, for example, threshold logarithms in Drell-Yan production. The soft-rapidity correspondence derived in [96–98] relates this quantity to the rapidity anomalous dimension. Our calculation of B_4 promotes a previous determination [99,100] of the four-loop rapidity anomalous dimension in terms of numerical constants to a fully analytical result, documented in the appendix.

The coefficients C_4 and D_4 in Eq. (12) are related to the lower-order cusp anomalous dimension, virtual anomalous dimension, and β-function coefficients through an all-order relation suggested in [39,41]. The explicit relations at four loops read

$$C_4 = 2A_1A_3 + A_2^2, \qquad D_4 = \sum_{l=1}^{3} A_l(B_{4-l} - \beta_{3-l}). \tag{14}$$

Both relations are fulfilled by our results.

Our analytical results also allow us to extract the behavior of the nonsinglet splitting functions in the limit $x \to 0$, stated in the appendix for $N_c = 3$. We observe that the logarithmically enhanced terms proportional to $\log^k x$ with $k = 6, 5$ for $P_{\rm ns}^{(3)+}$ agree with the expressions given in [101]. For $k = 4$, we find deviations proportional to ζ_2 in all five non-n_f color structures, which conspire to cancel in the leading-color limit.

In Fig. 3, we compare the nondistribution part [defined by omitting the terms proportional to $\delta(1-x)$ and arising from the subtraction at $x = 1$ originating from the plus distribution] of the nonsinglet splitting functions with $n_f = 4$ with the approximations provided in the `Fortran` code of Ref. [19]. We observe that overall the approximations agree well with the exact results at the level of the quoted uncertainties. Only $P_{\rm ns}^{(3)+}$ in the low-x region is slightly above the approximation's envelope.

Our analytic results allow us to construct simple power-logarithmic approximations, which contain only polynomials in $\{x, \log x, \log(1-x), \delta(1-x), [1/(1-x)]_+\}$. The constructed results have an accuracy better than 10^{-6} over the whole x range of $x \in (0,1)$ and can be used for more convenient numerical applications.

Finally, we used the correspondence [19] between spacelike and timelike nonsinglet anomalous dimensions, derived from reciprocity relations [41,102,103], to determine the four-loop nonsinglet timelike splitting functions, which are relevant to the scale evolution of fragmentation functions $D_i^h(x,\mu^2)$, describing the probability density for a

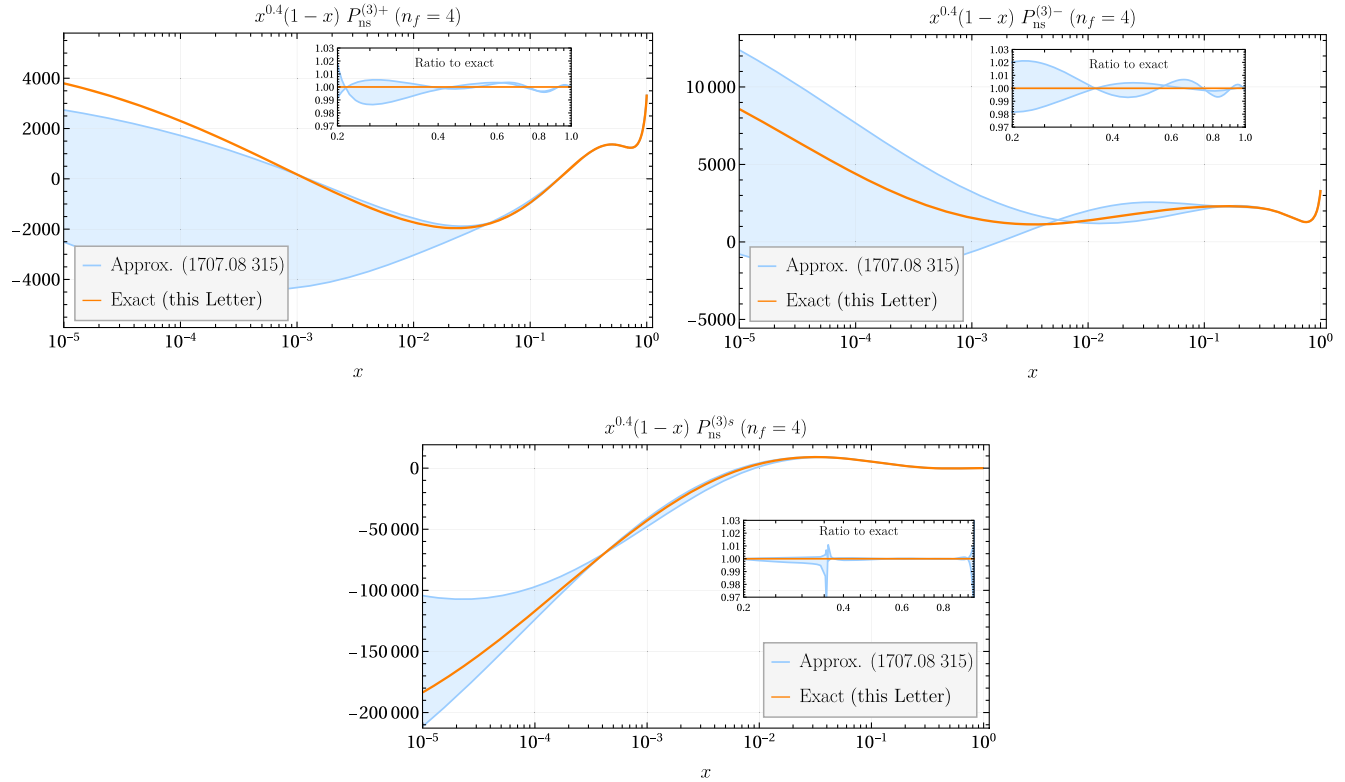


FIG. 3. The four-loop nonsinglet splitting functions $P_{\rm ns}^{(3)+}$, $P_{\rm ns}^{(3)-}$, and $P_{\rm ns}^{(3)s}$, evaluated for $n_f = 4$ and compared with approximations from Ref. [19]. All functions are multiplied by the factor $x^{0.4}(1-x)$ for presentation.

parton i to fragment into a hadron h carrying a momentum fraction x.

We provide all our analytical results as well as our numerical approximations in the Supplemental Material [104].

Summary and outlook—In this Letter, we derived the four-loop nonsinglet splitting functions in QCD in analytical form, based on a calculation of the anomalous dimensions of the nonsinglet operators for symbolic Mellin moment n. We provide results for both spacelike and timelike kinematics.

Our calculation confirms earlier partial results for the four-loop contributions involving closed fermion loops proportional to n_f^2 [27], n_f [29,31] and in the planar limit of QCD [19], as well as results for fixed values of $n \leq 16$ for the non-n_f terms [19,20] at four loops. Previously available approximations [19] to the four-loop nonsinglet splitting functions were based on the fixed-moment results. With the complete results obtained here, we show that these approximations are reliable within their quoted uncertainty band. Our newly derived results significantly reduce the uncertainties of the four-loop nonsinglet splitting functions, in particular for smaller values of x.

The analytic expressions can be used to study the limiting behavior of the four-loop nonsinglet splitting functions at $x \to 1$ and $x \to 0$, enabling systematic control not only on the logarithmically enhanced terms but also on power-suppressed contributions. From the $x \to 1$ behavior, we obtained exact values for the four-loop virtual and rapidity anomalous dimensions, which enter resummation at N^{4}LL.

Acknowledgments—We thank Andreas Vogt for enlightening discussions on the structure and implications of the results computed here. This work has been supported by the European Research Council (ERC) under the European Union's Horizon 2020 research and innovation program Grant Agreement No. 101019620 (ERC Advanced Grant TOPUP).

Data availability—The data that support the findings of this article are openly available at [105].

[1] J. D. Bjorken, Asymptotic sum rules at infinite momentum, Phys. Rev. **179**, 1547 (1969).
[2] J. D. Bjorken and E. A. Paschos, Inelastic electron proton and gamma proton scattering, and the structure of the nucleon, Phys. Rev. **185**, 1975 (1969).
[3] G. Altarelli and G. Parisi, Asymptotic freedom in parton language, Nucl. Phys. **B126**, 298 (1977).
[4] V. N. Gribov and L. N. Lipatov, Deep inelastic ep scattering in perturbation theory, Sov. J. Nucl. Phys. **15**, 438 (1972).
[5] Y. L. Dokshitzer, Calculation of the structure functions for deep inelastic scattering and e^+e^- annihilation by perturbation theory in quantum chromodynamics., Sov. Phys. JETP **46**, 641 (1977).
[6] D. J. Gross and F. Wilczek, Asymptotically free gauge theories. 2., Phys. Rev. D **9**, 980 (1974).
[7] H. D. Politzer, Asymptotic freedom: An approach to strong interactions, Phys. Rep. **14**, 129 (1974).
[8] E. G. Floratos, D. A. Ross, and C. T. Sachrajda, Higher order effects in asymptotically free Gauge theories: The anomalous dimensions of Wilson operators, Nucl. Phys. **B129**, 66 (1977); **B139**, 545(E) (1978).
[9] E. G. Floratos, D. A. Ross, and C. T. Sachrajda, Higher order effects in asymptotically free Gauge theories. II. Flavor singlet Wilson operators and coefficient functions, Nucl. Phys. **B152**, 493 (1979).
[10] A. Gonzalez-Arroyo, C. Lopez, and F. J. Yndurain, Second order contributions to the structure functions in deep inelastic scattering. I. Theoretical calculations, Nucl. Phys. **B153**, 161 (1979).
[11] G. Curci, W. Furmanski, and R. Petronzio, Evolution of parton densities beyond leading order: The nonsinglet case, Nucl. Phys. **B175**, 27 (1980).
[12] W. Furmanski and R. Petronzio, Singlet parton densities beyond leading order, Phys. Lett. **97B**, 437 (1980).
[13] R. Hamberg and W. L. van Neerven, The correct renormalization of the gluon operator in a covariant gauge, Nucl. Phys. **B379**, 143 (1992).
[14] S. Moch, J. A. M. Vermaseren, and A. Vogt, The three loop splitting functions in QCD: The nonsinglet case, Nucl. Phys. **B688**, 101 (2004).
[15] A. Vogt, S. Moch, and J. A. M. Vermaseren, The three-loop splitting functions in QCD: The singlet case, Nucl. Phys. **B691**, 129 (2004).
[16] J. Blümlein, P. Marquard, C. Schneider, and K. Schönwald, The three-loop unpolarized and polarized non-singlet anomalous dimensions from off shell operator matrix elements, Nucl. Phys. **B971**, 115542 (2021).
[17] J. Blümlein, P. Marquard, C. Schneider, and K. Schönwald, The three-loop polarized singlet anomalous dimensions from off-shell operator matrix elements, J. High Energy Phys. 01 (2022) 193.
[18] T. Gehrmann, A. von Manteuffel, and T.-Z. Yang, Renormalization of twist-two operators in covariant gauge to three loops in QCD, J. High Energy Phys. 04 (2023) 041.
[19] S. Moch, B. Ruijl, T. Ueda, J. A. M. Vermaseren, and A. Vogt, Four-loop non-singlet splitting functions in the planar limit and beyond, J. High Energy Phys. 10 (2017) 041.
[20] S. Moch, B. Ruijl, T. Ueda, J. A. M. Vermaseren, and A. Vogt, Low moments of the four-loop splitting functions in QCD, Phys. Lett. B **825**, 136853 (2022).
[21] G. Falcioni, F. Herzog, S. Moch, and A. Vogt, Four-loop splitting functions in QCD—The quark-quark case, Phys. Lett. B **842**, 137944 (2023).
[22] G. Falcioni, F. Herzog, S. Moch, and A. Vogt, Four-loop splitting functions in QCD—The gluon-to-quark case, Phys. Lett. B **846**, 138215 (2023).
[23] G. Falcioni, F. Herzog, S. Moch, A. Pelloni, and A. Vogt, Four-loop splitting functions in QCD—The quark-to-gluon case, Phys. Lett. B **856**, 138906 (2024).

[24] G. Falcioni, F. Herzog, S. Moch, A. Pelloni, and A. Vogt, Four-loop splitting functions in QCD—the gluon-gluon case–, Phys. Lett. B **860**, 139194 (2025).

[25] G. Falcioni, F. Herzog, S. Moch, A. Pelloni, and A. Vogt, Additional results on the four-loop flavour-singlet splitting functions in QCD, Phys. Lett. B **875**, 140278 (2026).

[26] J. A. Gracey, Anomalous dimension of nonsinglet Wilson operators at O (1/N(f)) in deep inelastic scattering, Phys. Lett. B **322**, 141 (1994).

[27] J. Davies, A. Vogt, B. Ruijl, T. Ueda, and J. A. M. Vermaseren, Large-nf contributions to the four-loop splitting functions in QCD, Nucl. Phys. **B915**, 335 (2017).

[28] T. Gehrmann, A. von Manteuffel, V. Sotnikov, and T.-Z. Yang, Complete N_f^2 contributions to four-loop pure-singlet splitting functions, J. High Energy Phys. 01 (2024) 029.

[29] T. Gehrmann, A. von Manteuffel, V. Sotnikov, and T.-Z. Yang, The $N_f C_F^3$ contribution to the non-singlet splitting function at four-loop order, Phys. Lett. B **849**, 138427 (2024).

[30] G. Falcioni, F. Herzog, S. Moch, J. Vermaseren, and A. Vogt, The double fermionic contribution to the four-loop quark-to-gluon splitting function, Phys. Lett. B **848**, 138351 (2024).

[31] B. A. Kniehl, S. Moch, V. N. Velizhanin, and A. Vogt, Flavor nonsinglet splitting functions at four loops in QCD: Fermionic contributions, Phys. Rev. Lett. **135**, 071902 (2025).

[32] B. A. Kniehl and V. N. Velizhanin, Four-loop anomalous dimension of flavor nonsinglet twist-two operator of general Lorentz spin in QCD: $\zeta(3)$ Term, Phys. Rev. Lett. **134**, 131901 (2025).

[33] J. McGowan, T. Cridge, L. A. Harland-Lang, and R. S. Thorne, Approximate N^{3}LO parton distribution functions with theoretical uncertainties: MSHT20aN^{3}LO PDFs, Eur. Phys. J. C **83**, 185 (2023); **83**, 302(E) (2023).

[34] A. Cooper-Sarkar, T. Cridge, F. Giuli, L. A. Harland-Lang, F. Hekhorn, J. Huston, G. Magni, S. Moch, and R. S. Thorne, A benchmarking of QCD evolution at approximate N^3LO, arXiv:2406.16188.

[35] R. D. Ball *et al.* (NNPDF Collaboration), The path to N^3LO parton distributions, Eur. Phys. J. C **84**, 659 (2024).

[36] T. Cridge *et al.*, Combination of aN^{3}LO PDFs and implications for Higgs production cross-sections at the LHC, J. Phys. G **52**, 065002 (2025).

[37] C. Hampson and M. Guzzi, DGLAP evolution at N3LO with the Candia algorithm, Phys. Rev. D **113**, 074008 (2026).

[38] A. Karlberg, P. Nason, G. Salam, G. Zanderighi, and F. Dreyer, HOPPET v2.0.0 release note, Eur. Phys. J. C **86**, 157 (2026).

[39] Y. L. Dokshitzer, G. Marchesini, and G. P. Salam, Revisiting parton evolution and the large-x limit, Phys. Lett. B **634**, 504 (2006).

[40] A. Mitov, S. Moch, and A. Vogt, Next-to-next-to-leading order evolution of non-singlet fragmentation functions, Phys. Lett. B **638**, 61 (2006).

[41] B. Basso and G. P. Korchemsky, Anomalous dimensions of high-spin operators beyond the leading order, Nucl. Phys. **B775**, 1 (2007).

[42] J. A. Dixon and J. C. Taylor, Renormalization of Wilson operators in gauge theories, Nucl. Phys. **B78**, 552 (1974).

[43] G. Falcioni and F. Herzog, Renormalization of gluonic leading-twist operators in covariant gauges, J. High Energy Phys. 05 (2022) 177.

[44] G. Falcioni, F. Herzog, S. Moch, and S. Van Thurenhout, Constraints for twist-two alien operators in QCD, J. High Energy Phys. 11 (2024) 080.

[45] T. Gehrmann, A. von Manteuffel, and T.-Z. Yang, Leading twist-two gauge-variant counterterms, Proc. Sci. **467**, 087 (2024).

[46] P. Nogueira, Automatic Feynman graph generation, J. Comput. Phys. **105**, 279 (1993).

[47] J. A. M. Vermaseren, New features of FORM, arXiv:math-ph/0010025.

[48] J. Davies, T. Kaneko, C. Marinissen, T. Ueda, and J. A. M. Vermaseren, FORM Version 5.0, arXiv:2601.19982.

[49] T. van Ritbergen, A. N. Schellekens, and J. A. M. Vermaseren, Group theory factors for Feynman diagrams, Int. J. Mod. Phys. A **14**, 41 (1999).

[50] J. Ablinger, J. Blümlein, A. Hasselhuhn, S. Klein, C. Schneider, and F. Wissbrock, Massive 3-loop ladder diagrams for quarkonic local operator matrix elements, Nucl. Phys. **B864**, 52 (2012).

[51] J. Ablinger, A. Behring, J. Blümlein, A. De Freitas, A. von Manteuffel, and C. Schneider, The 3-loop pure singlet heavy flavor contributions to the structure function $F_2(x, Q^2)$ and the anomalous dimension, Nucl. Phys. **B890**, 48 (2015).

[52] K. G. Chetyrkin, A. L. Kataev, and F. V. Tkachov, New approach to evaluation of multiloop Feynman integrals: The Gegenbauer polynomial x space technique, Nucl. Phys. **B174**, 345 (1980).

[53] S. Laporta, High precision calculation of multiloop Feynman integrals by difference equations, Int. J. Mod. Phys. A **15**, 5087 (2000).

[54] A. von Manteuffel and C. Studerus, Reduze 2—distributed Feynman integral reduction, arXiv:1201.4330.

[55] A. von Manteuffel and R. M. Schabinger, A novel approach to integration by parts reduction, Phys. Lett. B **744**, 101 (2015).

[56] T. Peraro, Scattering amplitudes over finite fields and multivariate functional reconstruction, J. High Energy Phys. 12 (2016) 030.

[57] M. Driesse, G. U. Jakobsen, G. Mogull, J. Plefka, B. Sauer, and J. Usovitsch, Conservative black hole scattering at fifth post-Minkowskian and first self-force order, Phys. Rev. Lett. **132**, 241402 (2024).

[58] X. Guan, X. Liu, Y.-Q. Ma, and W.-H. Wu, Blade: A package for block-triangular form improved Feynman integrals decomposition, Comput. Phys. Commun. **310**, 109538 (2025).

[59] Z. Bern, E. Herrmann, R. Roiban, M. S. Ruf, A. V. Smirnov, V. A. Smirnov, and M. Zeng, Amplitudes, supersymmetric black hole scattering at $\mathcal{O}(G^5)$, and loop integration, J. High Energy Phys. 10 (2024) 023.

[60] M. von Hippel and M. Wilhelm, Refining integration-by-parts reduction of Feynman integrals with machine learning, J. High Energy Phys. 05 (2025) 185.

[61] Z.-Y. Song, T.-Z. Yang, Q.-H. Cao, M.-x. Luo, and H. X. Zhu, Explainable AI-assisted optimization for Feynman integral reduction, J. High Energy Phys. 06 (2026) 225.

[62] F. Lange, J. Usovitsch, and Z. Wu, Kira 3: Integral reduction with efficient seeding and optimized equation selection, Comput. Phys. Commun. **322**, 109999 (2026).

[63] K. J. Larsen and Y. Zhang, Integration-by-parts reductions from unitarity cuts and algebraic geometry, Phys. Rev. D **93**, 041701 (2016).

[64] A. V. Smirnov and V. A. Smirnov, How to choose master integrals, Nucl. Phys. **B960**, 115213 (2020).

[65] J. Usovitsch, Factorization of denominators in integration-by-parts reductions, arXiv:2002.08173.

[66] S. Abreu, J. Dormans, F. Febres Cordero, H. Ita, and B. Page, Analytic form of planar two-loop five-gluon scattering amplitudes in QCD, Phys. Rev. Lett. **122**, 082002 (2019).

[67] M. Heller and A. von Manteuffel, MultivariateApart: Generalized partial fractions, Comput. Phys. Commun. **271**, 108174 (2022).

[68] T. Gehrmann and E. Remiddi, Differential equations for two loop four point functions, Nucl. Phys. **B580**, 485 (2000).

[69] J. M. Henn, Multiloop integrals in dimensional regularization made simple, Phys. Rev. Lett. **110**, 251601 (2013).

[70] J. Blümlein, M. Kauers, S. Klein, and C. Schneider, Determining the closed forms of the $O(\alpha_s^3)$ anomalous dimensions and Wilson coefficients from Mellin moments by means of computer algebra, Comput. Phys. Commun. **180**, 2143 (2009).

[71] J. Ablinger, A. Behring, J. Blümlein, A. De Freitas, A. von Manteuffel, and C. Schneider, Calculating three loop ladder and v-topologies for massive operator matrix elements by computer algebra, Comput. Phys. Commun. **202**, 33 (2016).

[72] R. N. Lee, A. V. Smirnov, and V. A. Smirnov, Solving differential equations for Feynman integrals by expansions near singular points, J. High Energy Phys. 03 (2018) 008.

[73] P. A. Baikov and K. G. Chetyrkin, Four loop massless propagators: An algebraic evaluation of all master integrals, Nucl. Phys. **B837**, 186 (2010).

[74] R. N. Lee, A. V. Smirnov, and V. A. Smirnov, Master integrals for four-loop massless propagators up to transcendentality weight twelve, Nucl. Phys. **B856**, 95 (2012).

[75] A. von Manteuffel and R. M. Schabinger, Planar master integrals for four-loop form factors, J. High Energy Phys. 05 (2019) 073.

[76] R. N. Lee, A. von Manteuffel, R. M. Schabinger, A. V. Smirnov, V. A. Smirnov, and M. Steinhauser, Master integrals for four-loop massless form factors, Eur. Phys. J. C **83**, 1041 (2023).

[77] J. A. M. Vermaseren, Harmonic sums, Mellin transforms and integrals, Int. J. Mod. Phys. A **14**, 2037 (1999).

[78] J. Henn, B. Mistlberger, V. A. Smirnov, and P. Wasser, Constructing d-log integrands and computing master integrals for three-loop four-particle scattering, J. High Energy Phys. 04 (2020) 167.

[79] C. Bogner, S. Müller-Stach, and S. Weinzierl, The unequal mass sunrise integral expressed through iterated integrals on $\bar{\mathcal{M}}_{1,3}$, Nucl. Phys. **B954**, 114991 (2020).

[80] J. Ablinger, A computer algebra toolbox for harmonic sums related to particle physics, Master's thesis, Linz University, 2009, arXiv:1011.1176.

[81] J. Ablinger, Computer algebra algorithms for special functions in particle physics, Ph.D. thesis, Linz University, 2012, arXiv:1305.0687.

[82] E. Remiddi and J. A. M. Vermaseren, Harmonic polylogarithms, Int. J. Mod. Phys. A **15**, 725 (2000).

[83] T. Gehrmann and E. Remiddi, Numerical evaluation of harmonic polylogarithms, Comput. Phys. Commun. **141**, 296 (2001).

[84] D. Maitre, HPL, a mathematica implementation of the harmonic polylogarithms, Comput. Phys. Commun. **174**, 222 (2006).

[85] J. Vollinga and S. Weinzierl, Numerical evaluation of multiple polylogarithms, Comput. Phys. Commun. **167**, 177 (2005).

[86] E. G. Floratos, C. Kounnas, and R. Lacaze, Higher order QCD effects in inclusive annihilation and deep inelastic scattering, Nucl. Phys. **B192**, 417 (1981).

[87] G. P. Korchemsky and A. V. Radyushkin, Renormalization of the Wilson loops beyond the leading order, Nucl. Phys. **B283**, 342 (1987).

[88] J. M. Henn, G. P. Korchemsky, and B. Mistlberger, The full four-loop cusp anomalous dimension in $\mathcal{N} = 4$ super Yang-Mills and QCD, J. High Energy Phys. 04 (2020) 018.

[89] A. von Manteuffel, E. Panzer, and R. M. Schabinger, Cusp and collinear anomalous dimensions in four-loop QCD from form factors, Phys. Rev. Lett. **124**, 162001 (2020).

[90] G. Das, S.-O. Moch, and A. Vogt, Soft corrections to inclusive deep-inelastic scattering at four loops and beyond, J. High Energy Phys. 03 (2020) 116.

[91] B. Agarwal, A. von Manteuffel, E. Panzer, and R. M. Schabinger, Four-loop collinear anomalous dimensions in QCD and $N = 4$ super Yang-Mills, Phys. Lett. B **820**, 136503 (2021).

[92] V. Ravindran, J. Smith, and W. L. van Neerven, Two-loop corrections to Higgs boson production, Nucl. Phys. **B704**, 332 (2005).

[93] A. Idilbi, X.-d. Ji, and F. Yuan, Resummation of threshold logarithms in effective field theory for DIS, Drell-Yan and Higgs production, Nucl. Phys. **B753**, 42 (2006).

[94] L. J. Dixon, L. Magnea, and G. F. Sterman, Universal structure of subleading infrared poles in gauge theory amplitudes, J. High Energy Phys. 08 (2008) 022.

[95] G. Falcioni, E. Gardi, and C. Milloy, Relating amplitude and PDF factorisation through Wilson-line geometries, J. High Energy Phys. 11 (2019) 100.

[96] Y. Li and H. X. Zhu, Bootstrapping rapidity anomalous dimensions for transverse-momentum resummation, Phys. Rev. Lett. **118**, 022004 (2017).

[97] A. A. Vladimirov, Correspondence between soft and rapidity anomalous dimensions, Phys. Rev. Lett. **118**, 062001 (2017).

[98] A. Vladimirov, Structure of rapidity divergences in multiparton scattering soft factors, J. High Energy Phys. 04 (2018) 045.

[99] I. Moult, H. X. Zhu, and Y. J. Zhu, The four loop QCD rapidity anomalous dimension, J. High Energy Phys. 08 (2022) 280.

[100] C. Duhr, B. Mistlberger, and G. Vita, Four-loop rapidity anomalous dimension and event shapes to fourth logarithmic order, Phys. Rev. Lett. **129**, 162001 (2022).
[101] J. Davies, C. H. Kom, S. Moch, and A. Vogt, Resummation of small-x double logarithms in QCD: Inclusive deep-inelastic scattering, J. High Energy Phys. 08 (2022) 135.
[102] Y. L. Dokshitzer and G. Marchesini, $N = 4$ SUSY Yang-Mills: Three loops made simple(r), Phys. Lett. B **646**, 189 (2007).
[103] H. Chen, T.-Z. Yang, H. X. Zhu, and Y. J. Zhu, Analytic continuation and reciprocity relation for collinear splitting in QCD, Chin. Phys. C **45**, 043101 (2021).
[104] See Supplemental Material at http://link.aps.org/supplemental/10.1103/sgtd-c4zg for electronic files containing the results of this article.
[105] T. Gehrmann *et al.*, The four-loop non-singlet splitting functions in QCD, arXiv:2604.09534.

End Matter

Four-loop rapidity anomalous dimension—Our result for the virtual anomalous dimension allows one to determine the analytical values of constants in the four-loop rapidity anomalous dimension that had previously been known only through numerical approximations. Following the conventions of [99], the fully analytical result for the rapidity anomalous dimension for representation $r = \{F, A\}$ reads

$$\begin{aligned}
\gamma_3^r = {} & C_A^3 C_r \left\{ \frac{9671}{12}\zeta_7 + 216\zeta_5\zeta_2 + 355\zeta_4\zeta_3 - \frac{20\,933}{36}\zeta_6 - \frac{5027}{9}\zeta_3^2 - \frac{45\,031}{27}\zeta_5 - \frac{6190}{9}\zeta_3\zeta_2 + \frac{2068}{9}\zeta_4 \right. \\
& \left. + \frac{301\,822}{81}\zeta_3 + \frac{395\,455}{486}\zeta_2 - \frac{28\,325\,071}{8748} \right\} \\
& + \frac{d_A^{abcd} d_r^{abcd}}{n_r} \left(1058\zeta_7 - 192\zeta_5\zeta_2 + 120\zeta_4\zeta_3 - \frac{1100}{3}\zeta_6 - \frac{440}{3}\zeta_3^2 - \frac{2680}{9}\zeta_5 - 8\zeta_4 + \frac{208}{9}\zeta_3 + 48\zeta_2 \right) \\
& + n_f C_A^2 C_r \left(\frac{247}{18}\zeta_6 - \frac{850}{9}\zeta_3^2 + \frac{1138}{27}\zeta_5 + \frac{404}{9}\zeta_3\zeta_2 - \frac{526}{9}\zeta_4 - \frac{32\,018}{81}\zeta_3 - \frac{41\,047}{243}\zeta_2 + \frac{11\,551\,831}{11\,664} \right) \\
& + n_f C_A C_F C_r \left(-8\zeta_6 + 156\zeta_3^2 - \frac{652}{3}\zeta_5 + \frac{152}{3}\zeta_3\zeta_2 - 100\zeta_4 - \frac{16\,819}{27}\zeta_3 - \frac{1741}{18}\zeta_2 + \frac{1\,870\,013}{1944} \right) \\
& + n_f C_F^2 C_r \left(100\zeta_6 + 40\zeta_3^2 + \frac{800}{3}\zeta_5 - 37\zeta_4 - \frac{2212}{9}\zeta_3 - \frac{21\,037}{216} \right) \\
& + n_f \frac{d_F^{abcd} d_r^{abcd}}{n_r} \left(\frac{400}{3}\zeta_6 + \frac{160}{3}\zeta_3^2 + \frac{800}{9}\zeta_5 + 16\zeta_4 - \frac{320}{9}\zeta_3 - 128\zeta_2 \right) \\
& + n_f^2 C_A C_r \left(\frac{368}{9}\zeta_5 + \frac{56}{9}\zeta_3\zeta_2 + \frac{40}{9}\zeta_4 - \frac{5564}{81}\zeta_3 + \frac{1688}{243}\zeta_2 - \frac{898\,033}{11664} \right) \\
& + n_f^2 C_F C_r \left(8\zeta_5 + \frac{40}{3}\zeta_4 + \frac{1732}{27}\zeta_3 - \frac{110\,059}{972} \right) + n_f^3 C_r \left(-\frac{4}{9}\zeta_4 + \frac{40}{9}\zeta_3 + \frac{2608}{2187} \right), \qquad \text{(A1)}
\end{aligned}$$

where n_r is the dimension of the representation with $n_r = N_c$ for the fundamental representation and $n_r = N_c^2 - 1$ for the adjoint representation.

Splitting functions in the small-x limit—To derive the limit $x \to 0$ of the nonsinglet splitting functions, we expand harmonic polylogarithms and rational functions in x. In QCD with $N_c = 3$, we obtain

$$\begin{aligned}
P_{\rm ns}^{(3)+} = {} & \frac{256}{729}\log^6 x + \left(\frac{3200}{243} - \frac{256}{243}n_f \right)\log^5 x + \left(-\frac{14\,240}{243}\zeta_2 + \frac{89\,008}{243} - \frac{7616}{243}n_f + \frac{64}{81}n_f^2 \right)\log^4 x \\
& + \left\{ \frac{1024}{243}\zeta_3 - \frac{85\,504}{81}\zeta_2 + \frac{1\,062\,692}{243} + \left(\frac{2368}{27}\zeta_2 - \frac{43\,208}{81} \right)n_f + \frac{4016}{243}n_f^2 - \frac{32}{243}n_f^3 \right\}\log^3 x \\
& + \left\{ \frac{362\,560}{81}\zeta_4 + \frac{55\,808}{81}\zeta_3 - \frac{1\,181\,128}{81}\zeta_2 + \frac{2\,763\,724}{81} + \left(-\frac{11\,264}{81}\zeta_3 + \frac{82\,096}{81}\zeta_2 - \frac{1\,010\,488}{243} \right)n_f \right.
\end{aligned}$$

$$+\left(-\frac{1472}{81}\zeta_2+\frac{103\,856}{729}\right)n_f^2-\frac{352}{243}n_f^3\Big\}\log^2 x+\Big\{-\frac{124\,160}{27}\zeta_5+\frac{59\,456}{27}\zeta_3\zeta_2+\frac{1\,222\,496}{81}\zeta_4$$
$$+\frac{479\,584}{81}\zeta_3-\frac{3\,824\,144}{81}\zeta_2+\frac{8\,777\,560}{81}+\left(-\frac{31\,904}{27}\zeta_4-\frac{68\,480}{81}\zeta_3+\frac{429\,088}{81}\zeta_2-\frac{3\,673\,924}{243}\right)n_f$$
$$+\left(\frac{128}{3}\zeta_3-\frac{9920}{81}\zeta_2+\frac{395\,972}{729}\right)n_f^2-\frac{256}{81}n_f^3\Big\}\log x+\frac{1\,912\,120}{243}\zeta_6+\frac{290\,320}{81}\zeta_3^2-\frac{2\,676\,784}{243}\zeta_5$$
$$+\frac{142\,720}{81}\zeta_3\zeta_2+\frac{3\,251\,956}{81}\zeta_4-\frac{19\,373\,648}{243}\zeta_2+\frac{1\,234\,960}{243}\zeta_3+\frac{39\,538\,148}{243}+\Big\{-\frac{11\,408}{9}\zeta_6$$
$$-\frac{2944}{9}\zeta_3^2+\frac{160\,352}{81}\zeta_5+\frac{35\,392}{81}\zeta_3\zeta_2-\frac{116\,504}{81}\zeta_4-\frac{356\,320}{81}\zeta_3+\frac{1\,883\,392}{243}\zeta_2-\frac{5\,427\,338}{243}\Big\}n_f$$
$$+\left\{-\frac{2528}{81}\zeta_4+\frac{40\,448}{243}\zeta_3-\frac{83\,168}{729}\zeta_2+\frac{430\,894}{729}\right\}n_f^2+\left(\frac{128}{81}\zeta_3-\frac{256}{243}\right)n_f^3+\mathcal{O}(x), \tag{B1}$$

$$P_{\rm ns}^{(3)-}=\frac{3632}{3645}\log^6 x+\left(\frac{22\,496}{1215}-\frac{1184}{1215}n_f\right)\log^5 x+\left(-\frac{21\,104}{243}\zeta_2+\frac{107\,168}{243}-\frac{8408}{243}n_f+\frac{80}{81}n_f^2\right)\log^4 x$$
$$+\left\{-\frac{16\,384}{243}\zeta_3-\frac{104\,960}{81}\zeta_2+\frac{1\,318\,516}{243}+\left(\frac{7744}{81}\zeta_2-\frac{50\,888}{81}\right)n_f+\frac{14\,288}{729}n_f^2-\frac{32}{243}n_f^3\right\}\log^3 x$$
$$+\left\{\frac{289\,040}{81}\zeta_4+\frac{2752}{9}\zeta_3+\frac{3\,326\,836}{81}-\frac{140\,024}{9}\zeta_2+\left(-\frac{17\,600}{81}\zeta_3+\frac{81\,488}{81}\zeta_2-\frac{14\,072}{3}\right)n_f\right.$$
$$\left.+\left(-\frac{448}{27}\zeta_2+\frac{37\,808}{243}\right)n_f^2-\frac{352}{243}n_f^3\right\}\log^2 x+\Big\{-\frac{899\,296}{81}\zeta_5+\frac{104\,960}{81}\zeta_3\zeta_2+\frac{2\,944\,304}{243}\zeta_4$$
$$+\frac{705\,760}{81}\zeta_3-\frac{11\,387\,728}{243}\zeta_2+\frac{28\,821\,224}{243}+\left(-\frac{3712}{3}\zeta_4-\frac{35\,008}{27}\zeta_3+\frac{131\,936}{27}\zeta_2-\frac{3\,736\,868}{243}\right)n_f$$
$$+\left(\frac{3584}{81}\zeta_3-\frac{27\,328}{243}\zeta_2+\frac{415\,300}{729}\right)n_f^2-\frac{256}{81}n_f^3\Big\}\log x+\frac{45\,400}{81}\zeta_6+\frac{325\,360}{81}\zeta_3^2+\frac{45\,184}{81}\zeta_3\zeta_2$$
$$-\frac{251\,216}{9}\zeta_5+\frac{4\,490\,708}{81}\zeta_4+\frac{174\,592}{9}\zeta_3-\frac{22\,420\,288}{243}\zeta_2+\frac{14\,570\,924}{81}+\Big\{-\frac{11\,408}{9}\zeta_6-\frac{2944}{9}\zeta_3^2$$
$$+\frac{20\,512}{9}\zeta_5+\frac{27\,968}{81}\zeta_3\zeta_2-\frac{181\,400}{81}\zeta_4-\frac{488\,320}{81}\zeta_3+\frac{1\,955\,552}{243}\zeta_2-\frac{5\,270\,602}{243}\Big\}n_f$$
$$+\left(-32\zeta_4+\frac{45\,824}{243}\zeta_3-\frac{80\,992}{729}\zeta_2+\frac{448\,622}{729}\right)n_f^2+\left(\frac{128}{81}\zeta_3-\frac{256}{243}\right)n_f^3+\mathcal{O}(x), \tag{B2}$$

$$\frac{P_{\rm ns}^{(3)s}}{n_f}=-\frac{152}{81}\log^6 x+\left(\frac{128}{81}-\frac{32}{81}n_f\right)\log^5 x+\left(\frac{3640}{81}\zeta_2-\frac{7360}{81}-\frac{160}{27}n_f\right)\log^4 x+\Big\{\frac{40\,000}{81}\zeta_3$$
$$+\frac{9920}{81}\zeta_2-\frac{77\,600}{81}+\left(\frac{320}{81}\zeta_2-\frac{320}{27}\right)n_f\Big\}\log^3 x+\Big\{\frac{88\,760}{27}\zeta_4+\frac{88\,480}{27}\zeta_3-\frac{2720}{27}\zeta_2$$
$$-\frac{135\,680}{27}+\left(-\frac{640}{9}\zeta_3+\frac{640}{3}\zeta_2-\frac{8960}{27}\right)n_f\Big\}\log^2 x+\Big\{+\frac{86\,080}{9}\zeta_5-\frac{33\,920}{9}\zeta_3\zeta_2+\frac{19\,600}{9}\zeta_4$$
$$+\frac{267\,200}{27}\zeta_3+\frac{298\,240}{27}\zeta_2-\frac{733\,280}{27}+\left(-\frac{800}{27}\zeta_4+\frac{10\,240}{27}\zeta_3-\frac{4160}{27}\zeta_2-\frac{7360}{9}\right)n_f\Big\}\log x$$
$$-\frac{93\,500}{81}\zeta_6-\frac{33\,520}{9}\zeta_3^2+\frac{213\,760}{27}\zeta_5-\frac{283\,840}{27}\zeta_3\zeta_2-\frac{672\,320}{9}+\frac{461\,120}{27}\zeta_4+\frac{1\,031\,920}{27}\zeta_3+\frac{622\,720}{27}\zeta_2$$
$$+\left(-\frac{12\,160}{27}\zeta_5+\frac{3200}{9}\zeta_3\zeta_2-\frac{4160}{27}\zeta_4-\frac{8000}{9}\zeta_3+\frac{17\,440}{27}\zeta_2-\frac{33\,920}{27}\right)n_f+\mathcal{O}(x). \tag{B3}$$

The results for a generic gauge group can be found in the Supplemental Material [104].